Letter

# Quantitative uncertainty metric to assess continuum breakdown for nonequilibrium hydrodynamics

Narendra Singh [1,*] and Michael Kroells[2]

[1]*Department of Mechanical Engineering, Stanford University, Stanford, California 94305, USA*

[2]*Department of Aerospace Engineering and Mechanics, University of Minnesota, Minneapolis, Minnesota 55455, USA*

(Received 9 July 2021; accepted 15 October 2021; published 23 November 2021)

We derive a metric to assess the reliability of linear constitutive relations that describe nonequilibrium hydrodynamic transport. The derivation of the metric utilizes the first-order perturbation to equilibrium Maxwellian velocity density function in the Chapman-Enskog expansion. The metric is defined as the contribution to macroscopic quantities from those regions of phase-space volume wherein the first-order perturbation becomes unphysical. The volume of these subregions of phase-space and, therefore, the corresponding contribution to macroscopic quantities increases with the strength of nonequilibrium (equivalently, the gradients of physical observables). Physical interpretation and performance of the metric are examined for a nonreactive sonic boundary layer flow. The metric provides the first *apriori* estimate of uncertainties on physical observables computed from the Navier-Stokes equations. The assigned uncertainties can be propagated in the flow field to assess the applicability of the Navier-Stokes equations for flows with strong nonequilibrium and/or rarefied gas physics.

DOI: 10.1103/PhysRevFluids.6.L111401

*Introduction.* In this Letter, we propose a simple metric to assess the breakdown of linear constitutive relations which model the nonequilibrium transport in hydrodynamics. In addition to quantifying the degree of nonequilibrium, the metric is relevant for simulations of hydrodynamic nonequilibrium flows. Applications such as hypersonic flows [1], reentry flows [2], micro-nanoscale flows [3,4], and high-speed particle-laden flows [5] require high-fidelity simulation tools that are accurate at a range of length scales and timescales. For example, hypersonic flow simulations include modeling strongly coupled nonequilibrium transport between macroscopic and molecular scales [6,7]. To resolve these multiscale physical phenomena containing strong gradients in physical observables, simulation tools require hybrid approaches.

Typically, a hybrid method couples a continuum fluid solver to a kinetic-scale tool such as a direct simulation Monte Carlo simulator (DSMC) [8,9]. The Navier-Stokes equations govern the flow physics in the continuum regions and the particle-based DSMC method is employed in the regions of the domain where the Navier-Stokes based solution becomes inaccurate. Although the DSMC method has been employed recently to simulate canonical turbulent flows [10], the computational cost of the DSMC method remains a bottleneck in vehicle-scale simulations, necessitating the need for hybrid-type methods. We propose a simple metric to identify nonequilibrium conditions under which transport modeled via the Navier-Stokes equations becomes *unreliable*, necessary for a computationally efficient hybrid method. This Letter also develops a framework to quantify

*narsingh@stanford.edu

 

uncertainties in quantities computed from the Navier-Stokes equations due to nonequilibrium modeling limitations.

This Letter first presents the kinetic theory that connects the Navier-Stokes equations and the microscopic description of a nonequilibrium gas using the Boltzmann equation. Then, state-of-the-art metrics are reviewed, and their key limitations are highlighted. Next, a generalized metric is derived and its physical interpretation is elucidated. The performance of the metric is examined using a nonreactive sonic boundary layer flow simulation. A framework for uncertainty quantification and corresponding implications for assessing the applicability of the Navier-Stokes equation are presented.

*Theory.* In a molecular description, the phase density function $[f(\boldsymbol{C})]$ times the differential phase-space volume $(d\boldsymbol{C})$ gives the probability of finding molecules moving within $\boldsymbol{C} \pm d\boldsymbol{C}/2$, where $\boldsymbol{C}$ is the peculiar velocity normalized by the most probable speed $C_{\mathrm{mp}}(=\sqrt{2k_BT/m})$, $k_B$ is the Boltzmann constant, $m$ is the molecular mass, and $T$ is the local temperature. The peculiar velocity is defined as $\boldsymbol{C} = \boldsymbol{c} - \mathbf{u}$, where $\boldsymbol{c}$ is the molecular velocity and $\mathbf{u}$ is the bulk (average) velocity of the gas.

For a single species, the nonequilibrium velocity distribution function $f$ obtained from the perturbation solution of the Boltzmann equation using the Chapman and Enskog series method [11] is

$$f = f_0(1 + \phi + \cdots), \tag{1}$$

where $f_0$ is the equilibrium distribution and $\phi$ is the first-order perturbation correction to model *small* deviations from equilibrium. The nondimensionalized equilibrium distribution $(f_0)$ is

$$f_0 = \frac{1}{\pi^{3/2}} \exp\left[-|\boldsymbol{C}|^2\right], \tag{2}$$

where $f_0$ is normalized using $[m/(2k_BT)]^{3/2}$. The macroscopic nondimensional density (1), the bulk velocity $(\boldsymbol{u})$, and the energy density $(e)$ of the gas are obtained by

$$\{1, \boldsymbol{u}, e\} = \int \{1, \boldsymbol{c}, |\boldsymbol{c}|^2\} f d\boldsymbol{C}, \tag{3}$$

and the expression for normalized $\phi$ is

$$\phi = \boldsymbol{q} \cdot \boldsymbol{C}\left(\frac{2}{5}|\boldsymbol{C}|^2 - 1\right) - \boldsymbol{\tau} : (\boldsymbol{C} \otimes \boldsymbol{C}), \tag{4}$$

where $\otimes$ is dyadic product and ":" is second-order contraction. The quantity $\boldsymbol{\tau}$ is the stress tensor and is normalized by $P$, where $P$ is pressure. The quantity $\boldsymbol{q}$ is the heat flux vector and is normalized by $(PC_{\mathrm{mp}}/2)$. The elements $\tau_{ij}$ and $q_i$ are given by

$$q_i = \frac{1}{2}\int C_i|\boldsymbol{C}|^2 f d\boldsymbol{C}, \quad \tau_{ij} = -\int C_iC_j f d\boldsymbol{C} - \delta_{i,j}. \tag{5}$$

To conserve mass, momentum, and energy, $\phi$ should satisfy the following collision invariant property:

$$\int \{1, \boldsymbol{c}, |\boldsymbol{c}|^2\}\phi f_0 d\boldsymbol{C} = \{0, 0, 0\}. \tag{6}$$

With this background, we now formally pose the question that we seek to address: when do the linear constitutive relationships ($q$ and $\tau$) obtained from $\phi$, valid for small deviations from equilibrium, break down?

*Review of state-of-the-art metrics.* We briefly summarize state-of-the-art metrics proposed to assess the breakdown of linear constitutive relations. Bird [12] proposed the ratio of the logarithm of the local time derivative of density to the collision frequency of molecules as a metric of assessing the breakdown of the Navier-Stokes equations. This metric is relevant for expanding flows, where

fewer intermolecular collisions prevent gas from establishing equilibrium. A more general criterion, known as the gradient-length Knudsen number ($\mathrm{Kn}_{\mathrm{gl}}$), which is proportional to the higher-order perturbation terms in Eq. (1) and is valid for gas undergoing compression and expansion is [13]

$$\mathrm{Kn}_{\mathrm{gl}-Q} = \left| \frac{\lambda}{Q} \frac{\partial Q}{\partial x} \right|, \tag{7}$$

where $Q$ is the local density, $\lambda$ is the local mean-free path, and the subscript gl denotes the gradient length. The metric has been generalized to include additional physical quantities for $Q = \rho$, $u$, and $T$ in Eq. (7). Whenever the maximum of $\mathrm{Kn}_{\mathrm{gl}-Q}$ is greater than 0.05 for any $Q$, Navier-Stokes equations are *considered* to break down [13]. Garcia and Alder [14,15] proposed the maximum of normalized stress tensor and the heat flux vector as other plausible metrics. These metrics ignore that the thermodynamic gradients may collectively, as opposed to a single maximum gradient, can drive the gas sufficiently far away from equilibrium.

Another metric that approximately incorporates the integrated effect of various thermodynamic gradients is the L-2 norm ($\|\phi\|$) of the perturbation [16], which is given by

$$\|\phi\| = \left[ \int \phi^2 f_0 d\boldsymbol{C} \right]^{1/2}. \tag{8}$$

Recently, Swaminathan-Gopalan *et al.* [17] have extended the formulation to include additional gradients such as multitemperatures for internal energy modes and multispecies diffusion using a generalized Chapman-Enskog expansion. Similar to $\mathrm{Kn}_{\mathrm{gl}}$, a value of $\|\phi\| > 0.05$ has been suggested as the indicator of the breakdown of the continuum assumption. Levermore *et al.* [18] proposed a non-negative definite matrix via a suitable moment of the distribution function, which can be evaluated based on Navier-Stokes solutions. The deviation of eigenvalues of this matrix from unity indicates the validity of the Navier-Stokes equations, and in this manner the proposed metric is not based on a particular benchmark problem.

The aforementioned metrics have a few limitations. The first limitation can be understood using the Boltzmann $H$ theorem, which provides entropy production via functional $H$ as

$$\frac{\partial H}{\partial t} = \frac{\partial}{\partial t} \int \ln(f) f d\boldsymbol{c} = \frac{\partial}{\partial t} \int \ln\left[f_0(1+\phi)\right] f_0(1+\phi) d\boldsymbol{c}. \tag{9}$$

Assuming $\phi$ is small, an approximation of Eq. (9) yields

$$\frac{\partial H}{\partial t} \approx \frac{\partial}{\partial t} \int \left[f_0\phi + \phi^2 f_0\right] d\boldsymbol{c} = \frac{\partial}{\partial t} \int \phi^2 f_0 d\boldsymbol{c} = \frac{\partial}{\partial t} \|\phi\|^2. \tag{10}$$

Therefore, $\|\phi\|$, intended to measure *large deviations* from equilibrium is a measure of $H$ functional ($\propto$ entropy) under the assumption of *small* $\phi$.

Second, the upper bound (0.05) for $\|\phi\|$ is empirical and is assigned using the comparisons of Navier-Stokes solutions and the DSMC method for hypersonic flow simulations over spherical geometry [13]. This means that setting the bound of 0.05 requires *a priori* knowledge of accurate solutions.

Third, the metric in $\|\phi\|$ corresponds to the zeroth-order moment of the perturbation. The low- and high-energy molecules that have insignificant contributions to the zeroth-order moment ($\|\phi\|$) can have significant contributions to the higher-order moments. These higher-order moments give rise to thermodynamic fluxes, which can no longer be accurately described by linear functions of forces. In the next section, we derive a metric which addresses these limitations.

*Proposed metric: Derivation and physical interpretation.* Before we derive our metric, we consider an example of a heat transfer problem, driven purely by a temperature gradient. The objective is to elucidate the relevant information that $\phi$ encodes related to the breakdown of linear constitutive relationships. Assuming that gradients in all other variables are absent, $\phi$ in Eq. (4)

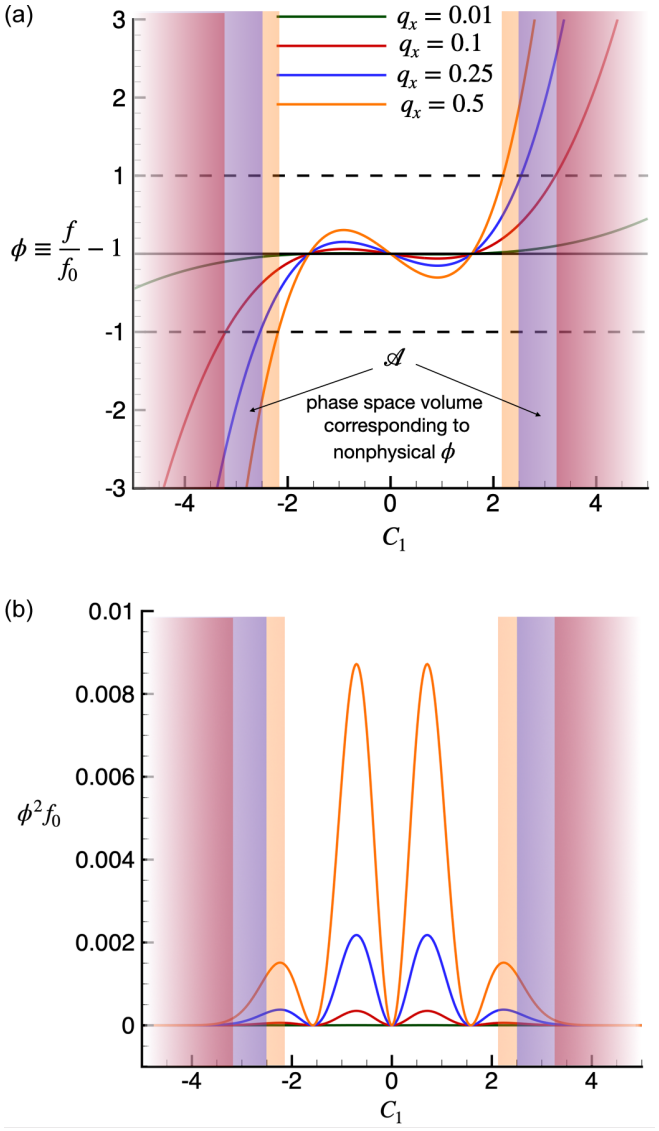


FIG. 1. (a) Variation of $\phi$ with $C_1$ for a range of heat fluxes ($q_x$) indicating regions in the phase space ($\mathcal{A}$) where $\phi$ is unphysical. (b) Variation of $\phi^2 f_0$ with $C_1$ for a range of $q_x$ showing vanishing contribution of $\mathcal{A}$ to $\|\phi\|$ [see Eq. (8)]. $C_2$ and $C_3$ are set as zero.

reduces to

$$\phi = q_x C_1 \left( \frac{2}{5} \boldsymbol{C}^2 - 1 \right), \tag{11}$$

where $q_x (\equiv q_1)$ is the heat flux in the $x$ direction. Figure 1(b) shows the variation of $\phi$ as a function of $C_1$ for a range of values of $q_1$. The perturbation ($\phi$) in the phase density function ($f$) in Eq. (1) cannot be less than $-1$ for $f(> 0)$ to be physical, implying

$$-1 \leqslant \phi \leqslant \phi_{\max}, \quad \text{where } \phi_{\max} \equiv 1. \tag{12}$$

As $\phi$ is the perturbation, its magnitude cannot be arbitrarily high and, therefore, should be small in comparison to unity. In this Letter we conservatively choose the upper bound $\phi_{\max}$ to be unity. Whenever $\phi$ lies outside the bounds in Eq. (12), $\phi$ is considered *unphysical*.

Figure 1(a) shows that as $q_x$ increases, the subvolume of the phase space in which $\phi$ violates the constraint in Eq. (12), shown by the regions in orange, blue, and red, increases. This increase in the phase-space volume as the gradients increase is the property that forms the core of the proposed metric. We also show that the unphysical regions contribute relatively insignificantly to the metric $\|\phi\|$. This can be concluded from observing the variation of the integrand in the metric $\|\phi\|$, i.e., $\phi^2 f_0$ with $C_1$ in Fig. 1(b). The quantity $\phi^2 f_0$ becomes vanishingly small at large values of $C_1$, where $\phi$ is unphysical, due to the Maxwell-Boltzmann weighting factor ($f_0$). Therefore, as laid out in the next section, the proposed metric does not rely on the magnitude of $\|\phi\|$, which may be small, but the regions in the phase space where $\phi$ takes *unphysical* can be significant in volume.

*Derivation and physical interpretation.* We define a probability ($\mathcal{P}$) of observing nonequilibrium gas in the phase-space subvolume ($\mathcal{A}$), which lies outside the constraint in Eq. (12), as

$$\mathcal{P} = \int_{\boldsymbol{C}\in\mathcal{A}} f d\boldsymbol{C} \approx \int_{\boldsymbol{C}\in\mathcal{A}} f_0 d\boldsymbol{C}, \tag{13}$$

$$\text{where } \mathcal{A} = \{C_1, C_2, C_3 \mid \phi \notin [-1, 1]\}. \tag{14}$$

$\mathcal{A}$ is that subvolume of the phase space in which $f = f_0(1+\phi)$ becomes unphysical. $\mathcal{P}$ measures the probability of finding the gas in $\mathcal{A}$. Note that $\mathcal{P}$ is equivalent to a fraction of the normalized density ($\rho = \int f_0 d\boldsymbol{C}$). Knowing this, we can define the density $\tilde{\rho}$, having a *reliable* component and an uncertainty estimate based on the computed density $\rho$, as

$$\tilde{\rho} = (1-\mathcal{P})\rho \ \pm \mathcal{P}\rho. \tag{15}$$

Equation (15) suggests that $\mathcal{P}$ adds uncertainty to the density, which increases with the degree of nonequilibrium. Therefore, we propose $\mathcal{P}$ as a rigorous metric of the breakdown of linear constitutive relationships.

The uncertainty estimates can also be applied to higher-order moments. A generalized metric which accounts for the contribution of $\mathcal{A}$ to other physical quantities can be obtained by

$$\langle \delta\psi \rangle = \int_{\boldsymbol{C}\in\mathcal{A}} \psi f_0 d\boldsymbol{C}, \tag{16}$$

where $\psi$ is an element of the vector $\boldsymbol{\Psi} = \{1, C_i, C^2, C_iC_j, C_iC^2, \phi^2\}$, $\langle \delta\psi \rangle$ is an element of the corresponding vector of moments $\langle \delta\boldsymbol{\psi} \rangle = \{\delta\rho, \delta\rho u_i, \delta e, \delta\sigma_{ij}, \delta q_i, \delta s^2\}$, and $\delta$ indicates that these moments are estimated from the restricted phase space ($\mathcal{A}$). In physical terms, the elements of $\langle \delta\boldsymbol{\psi} \rangle$ correspond to the contribution of $\mathcal{A}$ to the density, momentum, internal energy, stresses, heat flux, and square of entropy of the gas.

It is important to note that the metric and higher-order moments depend only on the local macroscopic gradients ($\boldsymbol{q}$ and $\boldsymbol{\tau}$) computed in continuum simulations. Provided $\boldsymbol{q}$ and $\boldsymbol{\tau}$ are known, the integration in Eq. (16) can be performed analytically by finding analytical approximations of the tail of $\phi$. Otherwise, polynomial or neural network representations of $\mathcal{P}$ (and higher-order moments) as a function of $\boldsymbol{q}$ and $\boldsymbol{\tau}$ can also be computed. These precomputed mathematical representations can yield $\mathcal{P}$ for local $\boldsymbol{q}$ and $\boldsymbol{\tau}$ evaluated from the Navier-Stokes equations in a computationally efficient manner.

*Results and implications.* In this section, a sonic boundary layer over a flat plate is simulated using a continuum approach to investigate the performance of the proposed metric and is compared to the widely used breakdown metric ($\mathrm{Kn}_{\mathrm{gl}}$). We provide a physical interpretation using simulation results and draw an important implication for developing constitutive relationships. For simulating the boundary layer flow as shown in a schematic in Fig. 2(a), we use the self-similar compressible Blasius boundary layer equations, first proposed by Dorodnitsyn [19] and Howarth [20]. These equations provide a simple means for obtaining realistic boundary layer profiles at different levels

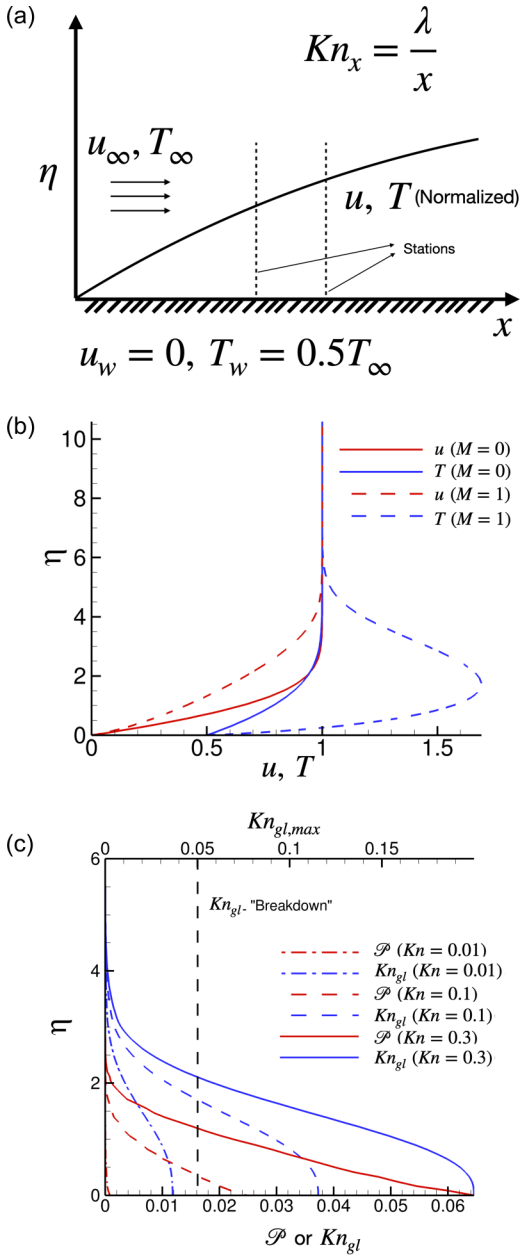


FIG. 2. (a) Sonic boundary layer simulation schematic, where stations correspond to different Kn values at which velocity and temperature normalized by free-stream values ($u_\infty$, $T_\infty$) are extracted. (b) Variation of velocity and temperature as a function of distance from the wall. (c) Variation of $\mathrm{Kn_{gl}}$ and the proposed metric as a function of distance from the wall.

of rarefaction. The free-stream flow speed ($u_\infty$) corresponds to a Mach number ($M$) of unity, and the free-stream temperature ($T_\infty$) is twice the wall temperature ($T_w$). We also simulate $M \approx 0$ as a reference case of small degrees of nonequilibrium. While velocity-slip and temperature-jump boundary conditions are consistent with the Navier-Stokes equations [21,22], for the sake of

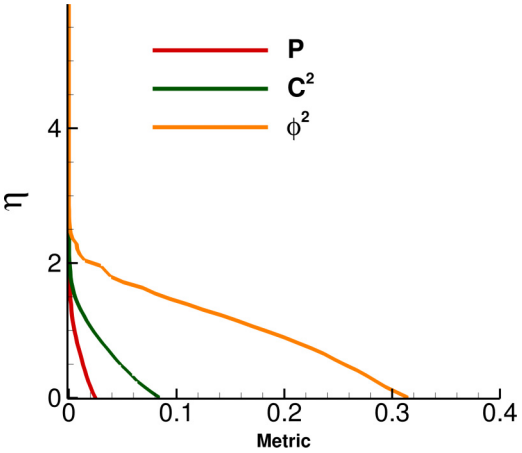


FIG. 3. Proposed metric ($\mathcal{P}$), temperature ($C^2$), and entropy production ($\phi^2$) variation with $\eta$ at Kn $= 0.1$.

simplicity, the no-slip boundary condition for velocity and the isothermal condition for temperature at the wall are employed. Although several simplifying assumptions such as ignoring chemical reactions, real gas effects, and slip-boundary condition effects are made in these simulations, these assumptions are reasonable for the presented analysis and correspondingly derived implications.

Figure 2(b) shows the simulation results for the two cases corresponding to $M = 0$ and $M = 1$. The figure shows the normalized velocity ($u$) and temperature ($T$) variations as a function of the normalized distance ($\eta$) from the wall. The magnitudes of the proposed metric and $\mathrm{Kn}_{\mathrm{gl}}$ are plotted in Fig. 2(c). As per the $\mathrm{Kn}_{\mathrm{gl}}$ criterion, the Navier-Stokes equations become invalid when $\mathrm{Kn}_{\mathrm{gl}} > 0.05$. Due to large gradients, the breakdown occurs primarily near the wall. Note that the slip-boundary condition will improve the Knudsen number regime in which Navier-Stokes equations are valid [22]. Here, the objective is to show that the trends of $\mathrm{Kn}_{\mathrm{gl}}$ qualitatively follow the proposed metric. Physically, $\mathrm{Kn}_{\mathrm{gl}}$ corresponds to a percentage change in a quantity over the length scale of a mean-free path. For example, $\mathrm{Kn}_{\mathrm{gl}-T} = 0.05$ can be interpreted as a 5% change in the temperature over a local mean-free path.

We next provide a physical interpretation of the proposed metric and related higher-order moments. The normalized density is unity [first element in Eq. (3)] and is equal to the integration of $f_0$ over the entire velocity space [also see Eq. (6)]. Consequently, $\mathcal{P}$ is equivalent to a fraction of the normalized density. A $\mathcal{P}$ of 0.05 implies that the computed density ($\rho$) has a reliable component of 0.95 times the computed density ($\rho$) with an uncertainty magnitude of $0.05\rho$. Therefore, we can define a physical observable, in this case the density $\tilde{\rho}$, containing the uncertainty estimate as $\tilde{\rho} = 0.95\rho \pm 0.05\rho$. Similarly, using Eq. (3) it can be easily shown that the bulk velocity ($u$) and the kinetic energy ($1/2u^2$) also have the same uncertainties as the density, i.e., $\tilde{u} = 0.95u \pm 0.05u$ and $(1/2)\tilde{u}^2 = 0.95(1/2)u^2 \pm 0.05(1/2)u^2$. Here $u$ is the computed velocity and $\tilde{u}$ is the corresponding proposed interpretation. Temperature ($T$) or thermal energy and entropy production, higher-order moments relative to density or momentum, has a larger uncertainty as shown in Fig. 3. In summary, the metric provides a rigorous framework of quantifying and propagating uncertainties on the computed magnitudes of physical observables from the Navier-Stokes equations.

*Conclusions.* We propose a simple metric to assess the degree of nonequilibrium, suggesting when physical observables obtained from the Navier-Stokes equations become unreliable. Unlike other metrics, the proposed metric does not rely on the *a priori* knowledge of accurate solutions to indicate the breakdown of Navier-Stokes equations. The mathematical framework helps us rigorously assign uncertainties to the physical observables computed from the Navier-Stokes equations. These uncertainty estimates can be propagated in fluid dynamic simulations to provide confidence intervals for computed quantities in a flow field. Last, while this Letter focused only on stresses

and the heat flux vector, other physical processes such as multitemperature gradients, diffusion, and chemical reactions can be included via a more generalized Chapman-Enskog expansion [17]. Such a generalization and applications of the metric to a broad range of flows including rigorous analysis using DSMC and computational fluid dynamics simulations comparisons, and comparisons to other metrics, would be desirable and interesting but are outside the scope of the current work.

[1] C. Park, Review of chemical-kinetic problems of future NASA missions. I-Earth entries, J. Thermophys. Heat Transfer **7**, 385 (1993).
[2] M. Ivanov and S. Gimelshein, Computational hypersonic rarefied flows, Annu. Rev. Fluid Mech. **30**, 469 (1998).
[3] K. Wu, Z. Chen, J. Li, X. Li, J. Xu, and X. Dong, Wettability effect on nanoconfined water flow, Proc. Natl. Acad. Sci. USA **114**, 3358 (2017).
[4] N. Kavokine, R. R. Netz, and L. Bocquet, Fluids at the nanoscale: From continuum to subcontinuum transport, Annu. Rev. Fluid Mech. **53**, 377 (2021).
[5] E. Ching, M. Barnhardt, and M. Ihme, Sensitivity of hypersonic dusty flows to physical modeling of the particle phase, J. Spacecr. Rockets **58**, 653 (2021).
[6] G. V. Candler, Rate effects in hypersonic flows, Annu. Rev. Fluid Mech. **51**, 379 (2019).
[7] N. Singh and T. Schwartzentruber, Consistent kinetic-continuum dissociation model. II. Continuum formulation and verification, J. Chem. Phys. **152**, 224303 (2020).
[8] G. A. Bird, *Molecular Gas Dynamics and the Direct Simulation of Gas Flows* (Clarendon Press, Oxford, 1994).
[9] I. D. Boyd and T. E. Schwartzentruber, *Nonequilibrium Gas Dynamics and Molecular Simulation* (Cambridge University Press, Cambridge, England, 2017).
[10] M. A. Gallis, N. P. Bitter, T. P. Koehler, J. R. Torczynski, S. J. Plimpton, and G. Papadakis, Molecular-Level Simulations of Turbulence and its Decay, Phys. Rev. Lett. **118**, 064501 (2017).
[11] S. Chapman and T. G. Cowling, *The Mathematical Theory of Non-uniform Gases: An Account of the Kinetic Theory of Viscosity, Thermal Conduction and Diffusion in Gases* (Cambridge University Press, Cambridge, England, 1990).
[12] G. Bird, Breakdown of translational and rotational equilibrium in gaseous expansions, AIAA J. **8**, 1998 (1970).
[13] I. D. Boyd, G. Chen, and G. V. Candler, Predicting failure of the continuum fluid equations in transitional hypersonic flows, Phys. Fluids **7**, 210 (1995).
[14] A. L. Garcia and B. J. Alder, Generation of the Chapman–Enskog distribution, J. Comput. Phys. **140**, 66 (1998).
[15] A. L. Garcia, J. B. Bell, W. Y. Crutchfield, and B. J. Alder, Adaptive mesh and algorithm refinement using direct simulation Monte Carlo, J. Comput. Phys. **154**, 134 (1999).
[16] S. Tiwari, Coupling of the Boltzmann and Euler equations with automatic domain decomposition, J. Comput. Phys. **144**, 710 (1998).
[17] K. Swaminathan-Gopalan, S. Subramaniam, and K. A. Stephani, Generalized Chapman-Enskog continuum breakdown parameters for chemically reacting flows, Phys. Rev. Fluids **1**, 083402 (2016).
[18] C. D. Levermore, W. J. Morokoff, and B. Nadiga, Moment realizability and the validity of the Navier–Stokes equations for rarefied gas dynamics, Phys. Fluids **10**, 3214 (1998).
[19] A. A. Dorodnitsyn, Boundary layer in a compressible gas, Prikl. Matem. Mekhan. **6**, 449 (1942).
[20] L. Howarth, Concerning the effect of compressibility on laminar boundary layers and their separation, Proc. R. Soc. London **194**, 16 (1948).
[21] R. MacCorrmack and D. Chapman, Computational fluid dynamics near the continuum limit, in *Proceedings of the 8th Computational Fluid Dynamics Conference* (AIAA Press, Reston, VA, 1987), pp. 87–1115.
[22] P. M. Bhide, I. Nompelis, T. Schwartzentruber, and G. Candler, Velocity-slip and temperature-jump effects in near-continuum hypersonic flows, AIAA J. **59**, 3815 (2021).